

***Insight-HXMT* firm detection of the highest energy fundamental cyclotron resonance scattering feature in the spectrum of GRO J1008-57**

M. Y. GE,¹ L. JI,² S. N. ZHANG,^{1,3} A. SANTANGELO,² C. Z. LIU,¹ V. DOROSHENKO,² R. STAUBERT,² J. L. QU,¹ S. ZHANG,¹ F. J. LU,¹ L. M. SONG,^{1,3} T. P. LI,^{1,4,3} L. TAO,¹ Y. P. XU,¹ X. L. CAO,¹ Y. CHEN,¹ Q. C. BU,¹ C. CAI,¹ Z. CHANG,¹ G. CHEN,¹ L. CHEN,⁵ T. X. CHEN,¹ Y. B. CHEN,⁴ Y. P. CHEN,¹ W. CUI,⁴ W. W. CUI,¹ J. K. DENG,⁶ Y. W. DONG,¹ Y. Y. DU,¹ M. X. FU,⁴ G. H. GAO,^{1,3} H. GAO,^{1,3} M. GAO,¹ Y. D. GU,¹ J. GUAN,¹ C. C. GUO,^{1,3} D. W. HAN,¹ Y. HUANG,¹ J. HUO,¹ S. M. JIA,¹ L. H. JIANG,¹ W. C. JIANG,¹ J. JIN,¹ Y. J. JIN,⁷ L. D. KONG,^{1,3} B. LI,¹ C. K. LI,¹ G. LI,¹ M. S. LI,¹ W. LI,¹ X. LI,¹ X. B. LI,¹ X. F. LI,¹ Y. G. LI,¹ Z. W. LI,¹ X. H. LIANG,¹ J. Y. LIAO,¹ B. S. LIU,¹ G. Q. LIU,⁶ H. W. LIU,¹ X. J. LIU,¹ Y. N. LIU,⁷ B. LU,¹ X. F. LU,¹ Q. LUO,^{1,3} T. LUO,¹ X. MA,¹ B. MENG,¹ Y. NANG,^{1,3} J. Y. NIE,¹ G. OU,¹ N. SAI,^{1,3} R. C. SHANG,⁶ X. Y. SONG,¹ L. SUN,¹ Y. TAN,¹ Y. L. TUO,^{1,3} C. WANG,⁸ G. F. WANG,¹ J. WANG,¹ L. J. WANG,¹ W. S. WANG,¹ Y. D. WANG,⁵ Y. S. WANG,¹ X. Y. WEN,¹ B. B. WU,¹ B. Y. WU,^{1,3} M. WU,¹ G. C. XIAO,^{1,3} S. XIAO,^{1,3} S. L. XIONG,¹ H. XU,¹ J. W. YANG,¹ S. YANG,¹ Y. J. YANG,¹ Y. J. YANG,¹ Q. B. YI,^{1,3} Q. Q. YIN,¹ Y. YOU,¹ A. M. ZHANG,¹ C. M. ZHANG,¹ F. ZHANG,¹ H. M. ZHANG,¹ J. ZHANG,¹ T. ZHANG,¹ W. C. ZHANG,¹ W. ZHANG,^{1,3} W. Z. ZHANG,⁵ Y. ZHANG,¹ Y. F. ZHANG,¹ Y. J. ZHANG,¹ Y. ZHANG,^{1,3} Z. ZHANG,⁸ Z. ZHANG,⁷ Z. L. ZHANG,¹ H. S. ZHAO,¹ X. F. ZHAO,^{1,3} S. J. ZHENG,¹ Y. G. ZHENG,⁹ D. K. ZHOU,^{1,3} J. F. ZHOU,⁷ R. L. ZHUANG,⁷ Y. X. ZHU,¹ AND Y. ZHU¹

¹Key Laboratory for Particle Astrophysics, Institute of High Energy Physics, Chinese Academy of Sciences, 19B Yuquan Road, Beijing 100049, China

²Institut für Astronomie und Astrophysik, Kepler Center for Astro and Particle Physics, Eberhard Karls, Universität, Sand 1, D-72076 Tübingen, Germany

³University of Chinese Academy of Sciences, Chinese Academy of Sciences, Beijing 100049, China

⁴Department of Astronomy, Tsinghua University, Beijing 100084, China

⁵Department of Astronomy, Beijing Normal University, Beijing 100088, China

⁶Department of Physics, Tsinghua University, Beijing 100084, People's Republic of China

⁷Department of Engineering Physics, Tsinghua University, Beijing 100084, China

⁸Key Laboratory of Space Astronomy and Technology, National Astronomical Observatories, Chinese Academy of Sciences, Beijing 100012, China

⁹College of physics Sciences & Technology, Hebei University, No. 180 Wusi Dong Road, Lian Chi District, Baoding City, Hebei Province, 071002 China

Submitted to ApJL

ABSTRACT

We report on the observation of the accreting pulsar GRO J1008-57 performed by *Insight-HXMT* at the peak of the source's 2017 outburst. Pulsations are detected with a spin period of 93.283(1)s. The pulse profile shows double peaks at soft X-rays, and only one peak above 20 keV. The spectrum is well described by the phenomenological models of X-ray pulsars. A cyclotron resonant scattering feature is detected with very high statistical significance at a centroid energy of $E_{\text{cyc}} = 90.32^{+0.32}_{-0.28}$ keV, for the reference continuum and line models, HIGHECUT and GABS respectively. Detection is very robust with respect to different continuum models. The line energy is significantly higher than what suggested from previous observations, which provided very marginal evidence for the line. This establishes a new record for the centroid energy of a fundamental cyclotron resonant scattering feature observed in accreting pulsars. We also discuss the accretion regime of the source during the *Insight-HXMT* observation.

Keywords: pulsars: individual (GRO J1008-57) — X-rays: binaries — stars: neutron — stars: magnetic field

1. INTRODUCTION

Accreting X-ray pulsars are neutron stars in binary systems, in which the strongly magnetised neutron star accretes matter from a donor star (typically a young O or B star). The magnetic fields of the neutron stars are thought to have strengths of $B \sim 10^{12}$ G. One of the most solid probes of the magnetic fields of accreting pulsars is the observation of cyclotron resonant scattering features (CRSFs). These scattering features appear as broad absorption lines observed in the source’s spectrum at hard X-ray energies corresponding to transitions between the discrete Landau levels of electrons’ motion perpendicular to the magnetic field lines. The first cyclotron line was discovered in 1976 in a balloon observation of Her X-1 (Trümper et al. 1977) and correctly interpreted by Truemper et al. (1978). Since then, CRSFs have been found in several tens of sources (for a recent review, see Staubert et al. 2019). Several systems exhibit harmonics in addition to the fundamental (see, e.g., Santangelo et al. 1999). The centroid energy of the fundamental and harmonic CRSF lines is given, in the non-relativistic approximation, by $E_{\text{cyc}} \sim 11.6 n B_{12} (1+z)^{-1}$ keV, where z is the gravitational redshift, B_{12} is the magnetic field in the line forming region in units of 10^{12} G, and n is the quantum number. In most X-ray pulsars, CRSF energies are observed to vary with the pulse phase, which is explained with the change of the view angle with respect to the line-forming region. In addition, the line energy has been observed to vary with the luminosity. A ‘positive’ correlation between the line centroid and the luminosity is observed for low luminosity sources. On the other hand, an anti-correlation, i.e., ‘negative’ correlation, has been observed for high luminosity sources (see, e.g., Staubert et al. 2007; Doroshenko et al. 2017; Vybornov et al. 2018). This is explained invoking different accretion regimes in the so-called sub-/super critical accretion (for details, see, e.g., Basko & Sunyaev 1976; Becker et al. 2012; Mushtukov et al. 2015).

GRO J1008-57 was discovered with the *Compton Gamma Ray Observatory (CGRO)/BATSE* during a bright outburst in 1993 (Stollberg et al. 1993). The distance to the source has been estimated to be 5.8 ± 0.5 kpc (Riquelme et al. 2012). GRO J1008-57 is a transient high mass X-ray binary (HMXB) with a Be companion. It exhibits periodic Type-I outbursts around the periastron passage, and sometimes irregular Type-II outbursts, which are brighter and longer. Bellm et al. (2014); Yamamoto et al. (2014) reported the marginal detection at $\sim 4\sigma$ of a CRSF line around 78 keV, by using non-simultaneous observations of *Swift*, *Suzaku* and *NuSTAR* taken during the 2012 outburst of the source. Other observations of different outbursts with CGRO and INTEGRAL hinted at a similar result but at even lower significance (Grove et al. 1995; Shrader et al. 1999; Kühnel et al. 2013; Wang 2014). In this paper, we report the highly significant detection of a CRSF in the spectrum of GRO J1008-57 at $E \sim 90$ keV. This is the highest energy fundamental CRSF ever observed. The line was observed during the outburst of GRO J1008-57 in 2017 with *Insight-HXMT*.

2. OBSERVATIONS AND RESULTS

The source was observed with *Insight-HXMT* for 50 ks at the peak of a Type-II outburst on 12th August 2017 (MJD 57977; see Figure 1, left panel). *Insight-HXMT* is the first Chinese X-ray astronomy satellite, launched on June 15, 2017 (Zhang et al. 2020). The instruments of the scientific payload include the high energy detectors (HE) (Liu et al. 2020), the medium energy detectors (ME) (Cao et al. 2020), and the low energy detectors (LE) (Chen et al. 2020), which have an effective area of 5100 cm^2 , 952 cm^2 and 384 cm^2 , respectively. We performed our analysis by using the HXMTSOFT¹ analysis package and the official user guides². The background was estimated and subtracted using the standalone python scripts LEBKGMAP, MEBKGMAP and HEBKGMAP (Li et al. 2020; Guo et al. 2020; Liao et al. 2020a,b). We screened the data according to the suggested criteria of the good-time-interval (GTI) selection: an elevation angle (ELV) larger than 10° ; geometric cutoff rigidity (COR) larger than 8 GeV; offset for the point position smaller than 0.1° ; at least 300 s before and after the South Atlantic Anomaly passage.

In the spectral analysis, we used the well-calibrated energy bands of LE, ME and HE: 2-10 keV, 8-30 keV and 30-135 keV, respectively. We searched for pulsations by using the Z_2^2 -test with a step of the Fourier frequency

¹ <http://www.hxmt.org/index.php/dataan>

² <http://www.hxmt.org/sjfxwd/65.jhtml>

(Buccheri et al. 1983), and by taking into account barycentric and orbital motion correction. We found that the source pulsates with a spin period of 93.283(1) s.

After folding the events, we obtained pulse profiles that clearly depend on the energy (shown in Figure 1, right panel). Similar as in other pulsars, the shape of the pulse profile is more complex in the low energy band, exhibiting double peaks, and gradually evolves into a single peak profile at higher energies.

For the spectral analysis, we fitted the wide-band phase-averaged spectrum with several phenomenological models typically used to model spectra of accreting pulsars (Staubert et al. 2019). We show here results from two of the models: the HIGHECUT model and the NPEX model (Mihara 1995).

The former is a product of a power-law model and a multiplicative exponential factor (Staubert et al. 2007):

$$I_E = \begin{cases} K \cdot E^{-\Gamma}, & \text{if } E \leq E_{\text{cut}} \\ K \cdot E^{-\Gamma} \exp\left(-\frac{E - E_{\text{cut}}}{E_f}\right), & \text{if } E \geq E_{\text{cut}} \end{cases}$$

Since the function contains a discontinuity of its first derivative, we included a smooth function, i.e., a weak Gaussian absorption line with the centre energy fixed to E_{cut} (for details, see, e.g., Coburn et al. 2002). The HIGHECUT model is widely used in the literature, and chosen as reference in the review article by Staubert et al. (2019) to model all spectra of the accreting pulsars with CRSFs. The NPEX model is a sum of positive and negative cutoff power-law spectral models, which resembles a Comptonization spectrum (Mihara 1995):

$$I_E = (K_1 \cdot E^{-\Gamma_1} + K_2 \cdot E^{+\Gamma_2}) \exp(-E/E_f)$$

where Γ_2 is normally fixed to 2 (Mihara 1995). The NPEX model is also largely used in literature, and for GRO J1008-57 allows a direct comparison of our findings with those of Yamamoto et al. (2014). Following earlier publications (Kühnel et al. 2013; Yamamoto et al. 2014; Bellm et al. 2014), a blackbody component at soft X-rays was included. In addition, we considered a Gaussian emission line around 6.4 keV to account for the K_α fluorescence iron line. All uncertainties quoted in this paper correspond to a 68% confidence level. Fits with the above defined continuum models were statistically not acceptable since they resulted in a reduced- $\chi^2 > 2$. In particular, significant residuals remained at hard X-rays (> 50 keV) (Figure 2).

We found that an additional absorption-like CRSF component, e.g., GABS or CYCLABS in XSPEC, improved the fits significantly, reaching a line significance in excess of 70 standard deviations (as found through Monte Carlo simulations SIMFTEST).³ The aforementioned GABS and CYCLABS models are widely used in the literature to describe CRSFs (Staubert et al. 2019; Mihara et al. 1990; Makishima et al. 1990). In particular the GABS model is the reference model used in the review by Staubert et al. (2019), while CYCLABS has been extensively used to model the CRSF in previous observations of GRO J1008-57. The two models are expressed as:

$$\text{GABS}(E) = \exp\left\{-\frac{D_{\text{cyc}}}{\sqrt{2\pi}\sigma_{\text{cyc}}}\exp\left[-\frac{1}{2}\left(\frac{E - E_{\text{cyc}}}{\sigma_{\text{cyc}}}\right)^2\right]\right\} \quad (1)$$

and

$$\text{CYCLABS}(E) = \exp\left\{-D_f \frac{(W_f E / E_{\text{cyc}})^2}{(E - E_{\text{cyc}})^2 + W_f^2}\right\} \quad (2)$$

We show the best fit spectra in Figure 2, and best fit results in Table 1. We observe that our findings on the line parameters do not significantly change when using other continuum models.

For completeness, we investigated the variability of the spectral shape with pulse phase. We obtained spectra for ten phase bins (see Figure 1), and analysed them using the aforementioned models. For some of the pulse phases, the parameters of the CRSF are not well constrained because of poor statistics. For these pulse phases, we have fixed the line width and depth at values obtained from the phase-averaged analysis. As an example, we show the spectral parameters change with the phase of the pulse in Figure 3, for the HIGHECUT plus GABS model. Both the CRSF and continuum parameters evolve with pulse phase significantly. The line energy varies with pulse phase up to ~ 5 keV (i.e., 6%) and in general shows a lower value around the pulse peak.

³ We simulated 1000 spectra using the best-fitting model where the CRSF is excluded, and then fitted these simulated spectra using the same model with and without the absorption. A distribution of $\Delta\chi^2$ can be obtained assuming that the CRSF is caused by statistical fluctuations. Thus the significance of the CRSF can be estimated by comparing the real observation with the simulated distribution.

3. DISCUSSION

We report on the spectral analysis of the outburst of GRO J1008-57 observed with *Insight-HXMT* in 2017. The spectral continuum is generally consistent with that reported in literature from observations of previous outbursts (Kühnel et al. 2013; Yamamoto et al. 2014; Bellm et al. 2014). In particular, we have observed with unprecedented high significance ($> 70\sigma$) a CRSF at $E_{\text{cyc}} = 90.32_{-0.28}^{+0.32}$ keV with a width (σ_{cyc}) of $14.57_{-0.11}^{+0.14}$ keV (combining the reference HIGHECUT and GABS models). The $E_{\text{cyc}}\text{-}\sigma_{\text{cyc}}$ relation is consistent with that of many other sources (see, Fig. 7 in Coburn et al. 2002).

This E_{cyc} is the highest value for any fundamental CRSF reported so far. The source’s magnetic field strength can be estimated to be $B = (1+z) E_{\text{cyc}}/11.6 = 7.8 \times 10^{12}(1+z)$ G, where z is the gravitational redshift at the line-forming region.

The line energy does not significantly depend on the choice of the continuum. However, it slightly changes (to $E_{\text{cyc}} = 83.00_{-0.63}^{+0.91}$) if the CYCLABS model is used, together with NPEX. This is not surprising since the true minimum of the CYCLABS line profile is lower by a factor of $1 + (\sigma_{\text{cyc}}/E_{\text{cyc}})^2$ if compared to the simple gaussian profile. The line energy deduced with CYCLABS can thus be lower up to 20%, compared to other models, especially when the line width is not well constrained, or actually frozen (Mihara 1995; Nakajima et al. 2010; Lutovinov et al. 2015).

The CRSF line energy observed by *Insight-HXMT*, is higher compared to the marginal (99% confidence limit) detection at $E_{\text{cyc}} = 76_{-1.7}^{+1.9}$ keV, reported by Yamamoto et al. (2014), based on *Suzaku* observations of the 2012 source’s outburst. The discrepancy can be explained considering that Yamamoto et al. (2014) modelled the data with the CYCLABS and NPEX models, and by the limited quality of *Suzaku* data at hard energies. Similar results at $\sim 4\sigma$ were obtained by Bellm et al. (2014), who modelled a combination of *Suzaku* and *NuSTAR* data with CYCLABS. The *Insight-HXMT* detection is also significantly higher than the hint of a CRSF reported by Kühnel et al. (2017) based on non-simultaneous *NuSTAR-Swift*, and *Suzaku* data at different epochs. Systematic uncertainties caused by the changes of the continuum spectrum were not taken into account, which might influence the line detection. Another source of discrepancy, might be related to the energy band used to model the broad-band spectrum, which is broader for our *Insight-HXMT* observation. We note, however, that our result is in agreement with *OSSE*’s observation of 1993 and the joint fit of the *RXTE* and *Suzaku* spectra (Kühnel et al. 2013), although these detections have a very low significance level (less than 2σ).

The bolometric luminosity during the *Insight-HXMT* observation in the energy range of 1-100 keV is $L_X \sim 5.8 \times 10^{37}$ erg s $^{-1}$, for a distance of 5.8 kpc (Riquelme et al. 2012), lower than that observed in 2012, $L_X \sim 1.1 \times 10^{38}$ erg s $^{-1}$, and comparable with observations reported by Kühnel et al. (2013).

On the base of our single observation, we cannot confirm or exclude whether the line centroid E_{cyc} varies with luminosity as reported by Yamamoto et al. (2014), who suggested that the CRSF energy could be negatively correlated with the luminosity like in the case of the two other accreting pulsars V 0332+53 and SMC X-2 (Tsygankov et al. 2006; Jaisawal & Naik 2016). If confirmed, the negative correlation would imply that the source is in the super-critical accretion regime (Basko & Sunyaev 1976), and the source luminosity must be higher than the critical luminosity L_{crit} .

Unfortunately, the comparison of our *Insight-HXMT* observation’s luminosity with predictions for L_{crit} found in literature is also inconclusive. According to Becker et al. (2012), L_{crit} is given by $\sim 1.5 \times 10^{37} B_{12}^{16/15}$ erg s $^{-1}$, that for our estimate of the B field implies $L_{\text{crit}} \sim 1.7 \times 10^{38}$ erg s $^{-1}$. The source would be therefore in the sub-Eddington accretion regime. On the other hand, predictions by Basko & Sunyaev (1976), and more recently by Mushtukov et al. (2015) (see their Figure 7), suggest lower values of the critical luminosity ($\lesssim 5 \times 10^{37}$ erg s $^{-1}$), comparable with the luminosity of our observation.

Bellm et al. (2014); Yamamoto et al. (2014) performed pulse-phase resolved spectroscopy on 2012 giant outburst data, but no significance dependence of the line parameters on the pulse phase was measured. For the *Insight-HXMT* observation discussed here, as it can be seen from Figure 3, the line energy appears to have a minimum at the peaks of the pulse profile, which is expected in the super-critical regime when an accretion column is present. In this case, the pulse maximum corresponds to a viewing angle, at which the largest fraction of the column, or of the neutron star’s surface illuminated by the column (Poutanen et al. 2013), is visible, since in this case, the line forming region includes the largest range of the magnetic field values. The field becomes in fact weaker both with the distance from the neutron stars surface, and towards the magnetic equator. The line width is expected to increase in this case, which does not appear to be the case, at least for the main peak. So no straightforward conclusion on the the accretion regime of the source can be obtained from the phase resolved analysis.

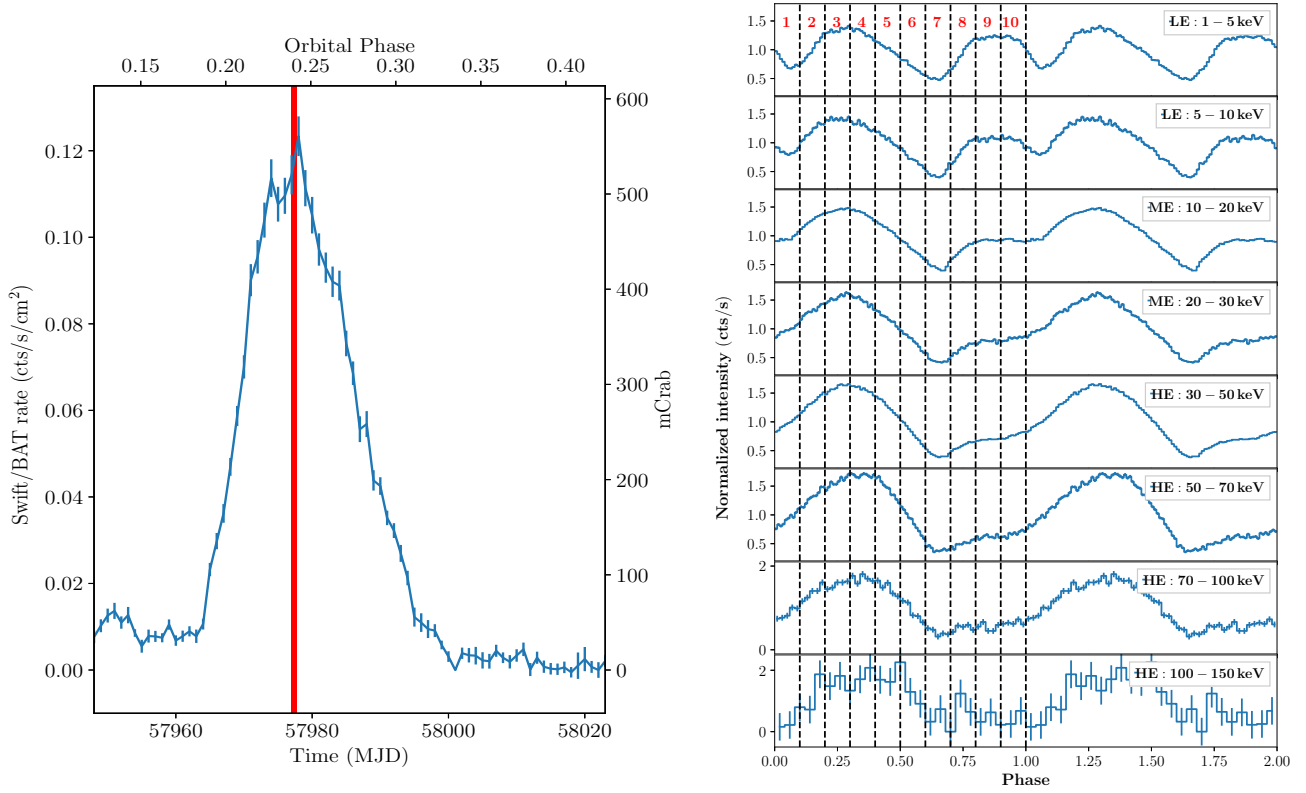


Figure 1. Left panel: The *Swift*/BAT lightcurve of GRO J1008-57 during its outburst in 2017. The red line represents the observational time of *Insight-HXMT*. The orbital phase is calculated based on the previously reported ephemeris Kühnel et al. (2013). Right panel: The pulse profiles in different energy bands of GRO J1008-57 around the outburst peak in 2017. The spin period is 93.283(1) s.

Establishing the accretion regime of the source (sub- or super-critical accretion) requires further observational studies of the luminosity dependence of the CRSF. A final answer regarding the critical luminosity of the source, and its accretion regime, can only be obtained through additional broad-band, high statistics observations of the source, both at lower and higher luminosity. These observations can provide significant measurements of the line parameters at different luminosity levels, obtained with the same instrument and using the same models. In addition, the monitoring of the source as a function of the luminosity can allow us to establish a break in the sign of the correlation between the line energy dependence and the luminosity, similar to that reported by Doroshenko et al. (2017); Vybornov et al. (2018). This letter shows that new *Insight-HXMT* observations can indeed solve the puzzle of the accretion regime of GRO J1008-57. It also shows the capability of the mission to discover CRSFs at energies higher than what accessible until now, and perhaps closer to the magnetic critical field.

ACKNOWLEDGMENTS

This work made use of the data from the *Insight-HXMT* mission, a project funded by China National Space Administration (CNSA) and the Chinese Academy of Sciences (CAS). The *Insight-HXMT* team gratefully acknowledges the support from the National Program on Key Research and Development Project (Grant No. 2016YFA0400800) from the Minister of Science and Technology of China (MOST) and the Strategic Priority Research Program of the Chinese Academy of Sciences (Grant No. XDB23040400). The authors thank supports from the National Natural Science Foundation of China under Grants No. 11503027, 11673023, 11733009, U1838201, U1838202, U1838104 and U1938103.

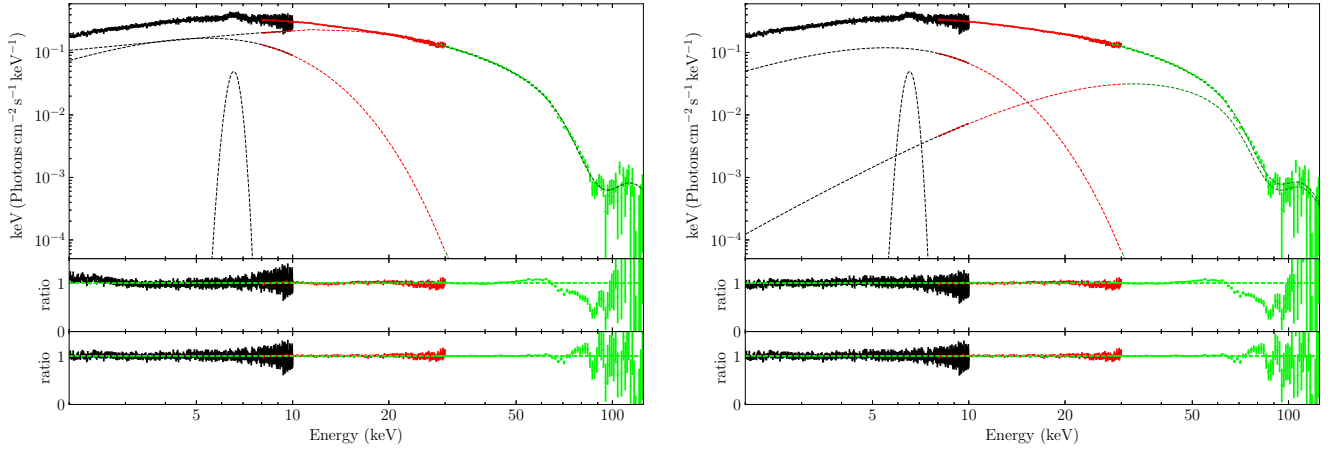


Figure 2. The unfolded phase-averaged spectrum of GRO J1008-57 observed in 2017 outburst fitted by HIGHECUT (left panel) and NPEX (right panel) models. The black, red and green lines represent LE, ME and HE energy ranges, respectively. We also show ratios, i.e., the data divided by the folded model, with and without the CRSF in the bottom and middle panels.

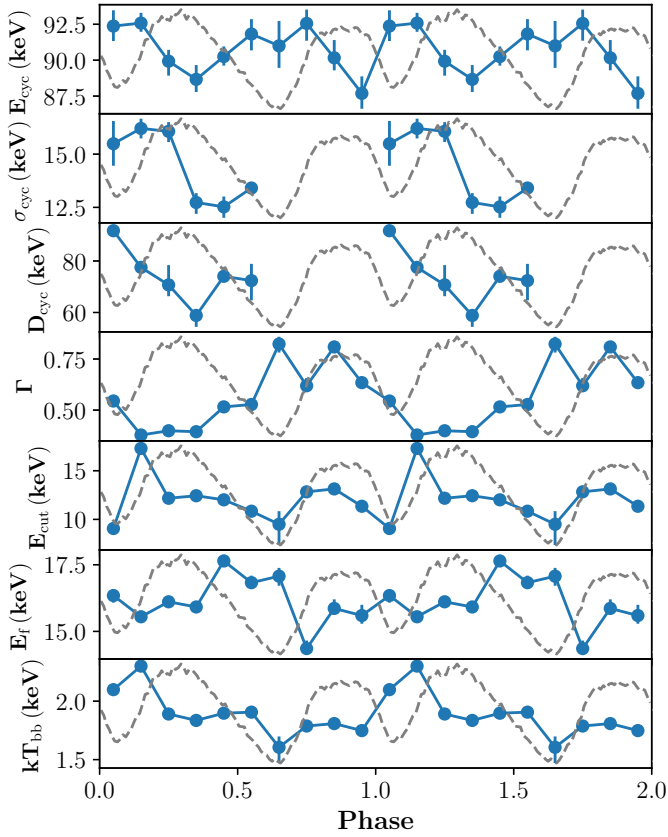


Figure 3. Phase-resolved spectral best fit parameters, obtained with the HIGHECUT and GABS models, superimposed onto the pulse profile in the energy range 1-5 keV. The line centroid appears to have a minimum around the profile peaks.

Table 1. Best-fitting parameters of GRO J1008-57 observed with *Insight-HXMT* in 2017.

	HIGHECUT		NPEX	
	GABS	CYCLABS	GABS	CYCLABS
E_{cyc} (keV)	$90.32^{+0.32}_{-0.28}$	$84.34^{+0.39}_{-0.43}$	$87.35^{+0.34}_{-0.37}$	$83.00^{+0.91}_{-0.63}$
σ_{cyc}/W_f (keV)	$14.57^{+0.14}_{-0.11}$	$15.48^{+0.14}_{-0.17}$	$12.42^{+0.09}_{-0.09}$	$14.51^{+0.98}_{-0.82}$
D_{cyc} (keV)/ D_f	$65.01^{+1.81}_{-1.58}$	$2.12^{+0.02}_{-0.02}$	$51.34^{+0.92}_{-0.70}$	$1.90^{+0.11}_{-0.11}$
kT_{bb} (keV)	$1.91^{+0.01}_{-0.01}$	$1.95^{+0.02}_{-0.02}$	$1.95^{+0.02}_{-0.01}$	$2.01^{+0.02}_{-0.02}$
Γ/Γ_1	$0.51^{+0.01}_{-0.01}$	$0.55^{+0.02}_{-0.01}$	$0.17^{+0.01}_{-0.01}$	$0.21^{+0.01}_{-0.01}$
E_f (keV)	$16.11^{+0.04}_{-0.04}$	$17.19^{+0.14}_{-0.09}$	$10.96^{+0.05}_{-0.04}$	$11.34^{+0.05}_{-0.09}$
E_{cut} (keV)	$10.87^{+0.07}_{-0.11}$	$12.10^{+0.66}_{-0.29}$	—	—
$C_{\text{ME/LE}}$	$1.00^{+0.01}_{-0.01}$	$0.99^{+0.01}_{-0.01}$	$0.99^{+0.01}_{-0.01}$	$0.98^{+0.01}_{-0.01}$
$C_{\text{HE/LE}}$	$0.99^{+0.01}_{-0.01}$	$0.98^{+0.01}_{-0.01}$	$0.99^{+0.01}_{-0.01}$	$0.97^{+0.01}_{-0.01}$
Reduced- χ^2 (dof)	1.11 (1375)	1.14 (1375)	1.12 (1377)	1.16 (1377)
Flux _{1–100} (erg/s/cm ²)	1.43×10^{-8}			

REFERENCES

- Basko, M. M., & Sunyaev, R. A. 1976, *MNRAS*, 175, 395, doi: [10.1093/mnras/175.2.395](https://doi.org/10.1093/mnras/175.2.395)
- Becker, P. A., Klochkov, D., Schönherr, G., et al. 2012, *Astron. & Astrophys.*, 544, A123, doi: [10.1051/0004-6361/201219065](https://doi.org/10.1051/0004-6361/201219065)
- Bellm, E. C., Fürst, F., Pottschmidt, K., et al. 2014, *ApJ*, 792, 108, doi: [10.1088/0004-637X/792/2/108](https://doi.org/10.1088/0004-637X/792/2/108)
- Buccheri, R., Bennett, K., Bignami, G. F., et al. 1983, *Astron. & Astrophys.*, 128, 245
- Cao, X., Jiang, W., Meng, B., et al. 2020, *Science China Physics, Mechanics, and Astronomy*, 63, 249504, doi: [10.1007/s11433-019-1506-1](https://doi.org/10.1007/s11433-019-1506-1)
- Chen, Y., Cui, W., Li, W., et al. 2020, *Science China Physics, Mechanics, and Astronomy*, 63, 249505, doi: [10.1007/s11433-019-1469-5](https://doi.org/10.1007/s11433-019-1469-5)
- Coburn, W., Heindl, W. A., Rothschild, R. E., et al. 2002, *ApJ*, 580, 394, doi: [10.1086/343033](https://doi.org/10.1086/343033)
- Doroshenko, V., Tsygankov, S. S., Mushtukov, A. e. A., et al. 2017, *MNRAS*, 466, 2143, doi: [10.1093/mnras/stw3236](https://doi.org/10.1093/mnras/stw3236)
- Grove, J. E., Kurfess, J. D., Philips, B. F., Strickman, M. S., & Ulmer, M. P. 1995, *International Cosmic Ray Conference*, 2, 1
- Guo, C.-C., Liao, J.-Y., Zhang, S., et al. 2020, arXiv e-prints, arXiv:2003.06260. <https://arxiv.org/abs/2003.06260>
- Jaisawal, G. K., & Naik, S. 2016, *MNRAS*, 461, L97, doi: [10.1093/mnras/461/L97](https://doi.org/10.1093/mnras/461/L97)
- Kühnel, M., Müller, S., Kreykenbohm, I., et al. 2013, *Astron. & Astrophys.*, 555, A95, doi: [10.1051/0004-6361/201321203](https://doi.org/10.1051/0004-6361/201321203)
- Kühnel, M., Fürst, F., Pottschmidt, K., et al. 2017, *A&A*, 607, A88, doi: [10.1051/0004-6361/201629131](https://doi.org/10.1051/0004-6361/201629131)
- Li, X., Li, X., Tan, Y., et al. 2020, arXiv e-prints, arXiv:2003.06998. <https://arxiv.org/abs/2003.06998>
- Liao, J.-Y., Zhang, S., Chen, Y., et al. 2020a, arXiv e-prints, arXiv:2004.01432. <https://arxiv.org/abs/2004.01432>
- . 2020b, arXiv e-prints, arXiv:2004.01432. <https://arxiv.org/abs/2004.01432>
- Liu, C., Zhang, Y., Li, X., et al. 2020, *Science China Physics, Mechanics, and Astronomy*, 63, 249503, doi: [10.1007/s11433-019-1486-x](https://doi.org/10.1007/s11433-019-1486-x)
- Lutovinov, A. A., Tsygankov, S. S., Suleimanov, V. F., et al. 2015, *MNRAS*, 448, 2175, doi: [10.1093/mnras/stv125](https://doi.org/10.1093/mnras/stv125)
- Makishima, K., Ohashi, T., Kawai, N., et al. 1990, *PASJ*, 42, 295
- Mihara, T. 1995, PhD thesis, , Dept. of Physics, Univ. of Tokyo (M95), (1995)
- Mihara, T., Makishima, K., Ohashi, T., Sakao, T., & Tashiro, M. 1990, *Nature*, 346, 250, doi: [10.1038/346250a0](https://doi.org/10.1038/346250a0)
- Mushtukov, A. A., Suleimanov, V. F., Tsygankov, S. S., & Poutanen, J. 2015, *MNRAS*, 447, 1847, doi: [10.1093/mnras/stu2484](https://doi.org/10.1093/mnras/stu2484)
- Nakajima, M., Mihara, T., & Makishima, K. 2010, *ApJ*, 710, 1755, doi: [10.1088/0004-637X/710/2/1755](https://doi.org/10.1088/0004-637X/710/2/1755)
- Poutanen, J., Mushtukov, A. A., Suleimanov, V. F., et al. 2013, *ApJ*, 777, 115, doi: [10.1088/0004-637X/777/2/115](https://doi.org/10.1088/0004-637X/777/2/115)
- Riquelme, M. S., Torrejón, J. M., & Negueruela, I. 2012, *A&A*, 539, A114, doi: [10.1051/0004-6361/201117738](https://doi.org/10.1051/0004-6361/201117738)
- Santangelo, A., Segreto, A., Giarrusso, S., et al. 1999, *ApJL*, 523, L85, doi: [10.1086/312249](https://doi.org/10.1086/312249)
- Shrader, C. R., Sutaria, F. K., Singh, K. P., & Macomb, D. J. 1999, *ApJ*, 512, 920, doi: [10.1086/306785](https://doi.org/10.1086/306785)

- Staubert, R., Shakura, N. I., Postnov, K., et al. 2007, *Astron. & Astrophys.*, 465, L25, doi: [10.1051/0004-6361:20077098](https://doi.org/10.1051/0004-6361:20077098)
- Staubert, R., Trümper, J., Kendziorra, E., et al. 2019, *Astron. & Astrophys.*, 622, A61, doi: [10.1051/0004-6361/201834479](https://doi.org/10.1051/0004-6361/201834479)
- Stollberg, M. T., Finger, M. H., Wilson, R. B., et al. 1993, *IAUC*, 5836, 1
- Truemper, J., Pietsch, W., Reppin, C., et al. 1978, *ApJL*, 219, L105, doi: [10.1086/182617](https://doi.org/10.1086/182617)
- Trümper, J., Pietsch, W., Reppin, C., & Sacco, B. 1977, in *Eighth Texas Symposium on Relativistic Astrophysics*, ed. M. D. Papagiannis, Vol. 302, 538, doi: [10.1111/j.1749-6632.1977.tb37072.x](https://doi.org/10.1111/j.1749-6632.1977.tb37072.x)
- Tsygankov, S. S., Lutovinov, A. A., Churazov, E. M., & Sunyaev, R. A. 2006, *MNRAS*, 371, 19, doi: [10.1111/j.1365-2966.2006.10610.x](https://doi.org/10.1111/j.1365-2966.2006.10610.x)
- Vybornov, V., Doroshenko, V., Staubert, R., & Santangelo, A. 2018, *Astron. & Astrophys.*, 610, A88, doi: [10.1051/0004-6361/201731750](https://doi.org/10.1051/0004-6361/201731750)
- Wang, W. 2014, *Research in Astronomy and Astrophysics*, 14, 565, doi: [10.1088/1674-4527/14/5/006](https://doi.org/10.1088/1674-4527/14/5/006)
- Yamamoto, T., Mihara, T., Sugizaki, M., et al. 2014, *Publications of the Astronomical Society of Japan*, 66, 59, doi: [10.1093/pasj/psu028](https://doi.org/10.1093/pasj/psu028)
- Zhang, S.-N., Li, T., Lu, F., et al. 2020, *Science China Physics, Mechanics, and Astronomy*, 63, 249502, doi: [10.1007/s11433-019-1432-6](https://doi.org/10.1007/s11433-019-1432-6)